QPE Algorithm for X-Band Dual Polarization Radar Applied in Guigang, China

Linyan HE, Jinfeng MENG, Junyu LONG, Jing LING, Yijin LIANG*

Guigang Meteorological Bureau, Guigang 537100, China

Abstract As an emerging meteorological detection tool, X-band dual polarization radar has gradually become an important means of radar quantitative precipitation estimation (QPE) due to its high spatial resolution and sensitivity. In this paper, utilizing the advantages of polarization parameters of dual polarization radar, the QPE product of Guigang X-band radar was optimized, and the optimized algorithm results were compared with the QPE products of surrounding Nanning and Yulin S-band radars. The results showed that the optimized method using polarization parameters of horizontal reflectance factor (Z_H) and differential reflectivity (Z_{DR}) had higher consistency between the QPE product of Guigang X-band radar and the measured precipitation of automatic weather stations. In terms of quantitative precipitation estimation, Guigang X-band radar was slightly inferior to Nanning and Yulin S-band radars.

Key words Dual polarization radar; QPE; Guigang

DOI 10.19547/j.issn2152 - 3940.2024.06.005

Quantitative precipitation estimation (QPE) is an important method for evaluating precipitation and its distribution in rainfall forecasting. Due to its limited spatial and temporal coverage capabilities at automatic weather stations, radar observation has become an indispensable tool for modern meteorological research and application[1-4]. X-band radar, as an emerging meteorological detection tool, has gradually become an important means of QPE research due to its high spatial resolution and sensitivity. Compared with S-band radar, X-band radar can more accurately capture small-scale precipitation phenomena. Especially in urban areas and complex terrains, this advantage is particularly evident.

With the development of meteorological monitoring technology in recent years, the demand for quantitative estimation of precipitation has been increasing. Especially in the context of frequent extreme weather events, accurate prediction of precipitation is of great significance for disaster prevention and reduction. Therefore, the quantitative precipitation estimation research through X-band radar can not only improve the accuracy of precipitation monitoring, but also provide more reliable data support for meteorological forecasting[5-11]. At present, there is relatively little research on quantitative precipitation estimation of X-band radar in China. Zhang Zhe *et al.*[12] studied the quantitative precipitation estimation puzzle system of Shenzhen S-band and X-band radars, and QPE product with a time resolution of 1 min and a spatial resolution of 30 m was produced. Mei Yufei *et al.*[13] used the QPE networking products of four X-band dual polarization phased array radars in Zhuhai and the hourly precipitation data of corresponding regional rainfall stations to evaluate the quality of phased array radar QPE products. Based on hourly precipitation data from 36 precipitation periods in Xiamen X-band phased array radar networking experiment, Xun Aiping *et al.*[14] used the optimization processing method to optimize four precipitation estimation methods applicable to S-band dual polarization radar, making them suitable for X-band phased array radar. As the first X-band dual polarization radar in Guangxi, the application of Guigang X-band dual polarization radar in quantitative precipitation estimation was explored in this paper. By comparing and evaluating the errors of different QPE algorithms, the locally applicable precipitation estimation method of X-band radar in Guigang was obtained, and the QPE product effect was evaluated. At the same time, it was compared and evaluated with the quantitative precipitation estimation of S-band radar. This paper can provide reference for quantitative precipitation estimation of other X-band weather radars in Guangxi.

1 Data and methods

1.1 Data Based on the study of multiple heavy precipitation processes in Guigang City in 2023, the used data in this paper included: hourly precipitation data of national meteorological stations and regional automatic meteorological stations around Guigang X-band, Nanning S-band, and Yulin S-band radars; the base data products of S-band radars in Nanning and Yulin, as well as the X-band dual polarization radar in Guigang, including horizontal reflectivity (Z_H), differential reflectivity (Z_{DR}), differential propagation phase shift rate (K_{DP}), correlation coefficient (CC), *etc.*

All meteorological data used in this paper came from the Guangxi Zhuang Autonomous Region Meteorological Information Center, and the base data product of Guigang X-band dual polarization radar came from the Guigang Meteorological Bureau.

Received: October 11, 2024 Accepted: November 30, 2024

Supported by Guangxi Meteorological Research Program Project (GUIQIKE 2023M28, GUIQIKE 2023M27, GUIQIKE 2023QN16).

* Corresponding author.

1.2 Methods

1.2.1 Precipitation estimation method. The conventional precipitation estimation method is based on the ZR relationship established between radar reflectivity factor and rainfall intensity. In this paper, relying on the advantages of polarization parameters of dual polarization radar, the three measured values Z_H, Z_{DR}, and K_{DP} of the radar were combined in different ways to estimate precipitation. There were three main methods for estimating precipitation using radar in this project (formulas 1 – 3).

$$R(Z_H) = a \cdot Z_H^b \tag{1}$$

$$R(K_{DP}) = a \cdot K_{DP}^b \tag{2}$$

$$R(Z_H, Z_{DR}) = a \cdot Z_H^b Z_{DR}^c \tag{3}$$

where $R(Z_H)$ shows the relationship between reflectivity factor Z_H and rainfall intensity; $R(K_{DP})$ shows the relationship between differential propagation phase shift rate K_{DP} and rainfall intensity; $R(Z_H, Z_{DR})$ shows the relationship among reflectivity factor Z_H, differential reflectivity Z_{DR} and rainfall intensity.

1.2.2 Determination of coefficients for the calculation formula of rainfall intensity R. The coefficients of the rainfall intensity calculation formula in this paper were quoted from QPE coefficient proposed by Ryzhkov *et al*[15]. In $R(Z_H) = a \cdot Z_H^b$, $a = 0.030\,6$, $b = 0.639$; in $R(K_{DP}) = a \cdot K_{DP}^b$, $a = 16.9$, $b = 0.801$; in $R(Z_H, Z_{DR}) = a \cdot Z_H^b Z_{DR}^c$, $a = 0.015$, $b = 0.790$, $c = -2.17$.

1.2.3 Error evaluation indicators. In order to objectively reflect the error between radar estimated precipitation and regional automatic weather station observed precipitation, the evaluation parameters of correlation coefficient CC, root mean square error $RMSE$, relative mean error RMB, and deviation $Bias$ were selected as the error evaluation indicators in this project. The calculation formula is as follows:

$$CC = \frac{\sum_{i=1}^{n}(R_i - R_{ave})(G_i - G_{ave})}{\sqrt{\sum_{i=1}^{n}(R_i - R_{ave})^2 \sum_{i=1}^{n}(G_i - G_{ave})^2}} \tag{4}$$

$$RMSE = \sqrt{\frac{1}{n}\sum_{i=1}^{n}(R_i - G_i)^2} \tag{5}$$

$$RMB = \frac{\sum_{i=1}^{n}(R_i - G_i)}{\sum_{i=1}^{n}G_i} \times 100\% \tag{6}$$

$$Bias = \frac{1}{n}\sum_{i=1}^{n}(R_i - G_i) \tag{7}$$

where R_i shows radar estimation of precipitation; R_{ave} shows the average value of all radar estimated precipitation samples; G_i shows hourly rainfall intensity observed by automatic weather stations; G_{ave} shows the average value of all hourly rainfall intensity samples; n is total sample size.

2 Research on quantitative precipitation estimation

2.1 Attenuation correction of X-band dual polarization radar Weather radar can detect strong convective weather such as thunderstorms and hail. But in practical applications, the attenuation effect of rain areas on radar echoes cannot be ignored. Due to the longer wavelength, S-band radar usually has better penetration ability when dealing with larger particles (water droplets, raindrops, *etc.*). This means that under poor precipitation or atmospheric conditions, the echo attenuation of S-band radar is relatively small, making it more effective for detecting moderate precipitation intensity. Due to its shorter wavelength, X-band radar experiences more severe attenuation in precipitation than S-band radar. Research has shown that the attenuation coefficient of X-band radar is 7 to 8 times higher than that of C-band and S-band radars, respectively. This means that X-band radar experiences more severe signal attenuation during detection, especially in areas with heavy precipitation. Therefore, when using X-band radar echo data, attenuation issues need to be considered, and ground object echoes also need to be processed. Ground object clutter can affect the quantitative measurement effectiveness of precipitation through radar, and ground object echoes must be processed before further processing of radar data. Due to the spatial discontinuity and large gradient of the reflectance factor Z_H and differential reflectance factor Z_{DR} of ground object clutter, ground object echoes can be identified based on this characteristic.

In this paper, the $A_H - K_{DP}$ empirical formula provided by Bringi *et al.* and empirical formula between A_H and Z_H proposed by Park *et al.* were used to correct the radar echoes of Guigang X-band radar[16-18]. At the same time, the spatial discontinuity of the reflectance factor Z_H and differential reflectance factor Z_{DR} of ground object clutter was utilized to identify ground object echoes.

In this paper, the above method was used to correct the echo of the X-band radar in Guigang. In Fig. 1, a convective precipitation data observed at a 1.5° elevation angle during a body scan starting at 03:06 on April 24, 2023 was analyzed. The original reflectivity factor of Guigang X-band radar was shown in Fig. 1a. Seen from Fig. 1a, the scattered rainfall echoes can be observed near the X-band radar in Guigang before correction. The reflectivity factors of most echoes were 20 – 30 dBz, with the strongest reflectivity factor being 40 – 50 dBz. After correction, the reflectivity factors of rainfall echoes observed by the Guigang X-band radar were significantly enhanced, mostly to 30 – 50 dBz, with the strongest reflectivity factor exceeding 50 dBz (Fig. 1b). Fig. 1c was the reflectance factor observed by Yulin S-band radar in the same area. By comparison, it can be seen that the rainfall echoes in the same area observed by the Guigang X-band had a larger range and stronger intensity after correction. However, the rainfall echoes in the range of 109° – 110° E and 22.0° – 22.5° N were closer to the Yulin S-band radar, and the rainfall echoes in this range were stronger than those observed by the Guigang X-band radar.

2.2 Error estimation of QPE algorithm The conventional precipitation estimation method is based on the ZR relationship established between radar reflectivity factor and rainfall intensity. In this paper, relying on the advantages of polarization parameters of Guigang X-band dual polarization radar, the three measured val-

ues Z_H, Z_{DR}, and K_{DP} of the radar were combined in different ways to optimize the conventional ZR relationship equation. According to formulas 1 – 3, the 1-h precipitation estimated by the QPE product was compared with the 1-h measured precipitation of automatic weather station. Among them, *CC* is a statistical indicator that reflects the consistency between the QPE product and the observed data of the automatic weather station. The higher the *CC*, the higher the consistency between the QPE product and the actual observed precipitation of the automatic weather station; *RMSE* is a statistical indicator that reflects the error between QPE and observed precipitation of automatic weather stations. The closer it is to 0, the smaller the error and the lower the dispersion of precipitation estimation. *RMB* is an indicator that reflects the average deviation situation. A positive (negative) *RMB* indicates that the QPE product overestimates (underestimates) the actual precipitation observed by the automatic weather stations. *Bias* is used to quantify the systematic deviation between estimated values and actual values.

In Fig. 2, the 1-h precipitation estimated by the QPE product of Guigang X-band radar was compared with the 1-h precipitation observed by the regional automatic weather station using three methods corresponding to formulas 1 – 3, hereinafter referred to as Method 1, Method 2, and Method 3. These three methods were used to evaluate all sample pairs within a 150 km range of the Guigang X-band radar in June and July 2023, with a total of 49 525 sample data pairs evaluated. The *RMSE* of the QPE product calculated according to Method 1 was 5.992, as shown in Fig. 2a. The *RMSE* of the QPE product calculated according to Method 2 was 5.457, as shown in Fig. 2b. The *RMSE* of the QPE product calculated according to Method 3 was 5.080, as shown in Fig. 2c, indicating that for the X-band radar in Guigang, the error between the QPE product of Method 3 and the actual precipitation measured by the automatic meteorological observation station was the smallest. From Fig. 2a, it can be seen that *CC* of the QPE product calculated according to Method 1 was 0.684. From Fig. 2b, it can be seen that *CC* of the QPE product calculated according to Method 2 was 0.691. From Fig. 2c, it can be seen that *CC* of the QPE product calculated according to Method 3 was 0.701. From the perspective of correlation coefficient, the QPE product coefficient of Method 3 was the highest, indicating that the QPE product of Method 3 had the best consistency with the observation data of automatic weather station for these three methods. Based on *RMB*, *RMB* of the QPE product calculated by Method 1 was –44.6%, as shown in Fig. 2a. *RMB* of the QPE product calculated by Method 2 was –30.8%, as shown in Fig. 2b. *RMB* of the QPE product calculated by Method 3 was –13.5%, as shown in Fig. 2c. It can be seen that the QPE products calculated by the three methods all underestimated the measured precipitation of regional automatic weather stations. The conventional Method 1 had the most severe underestimation, with a decrease of 44.6%. After optimizing Method 1 with the advantages of polarization parameters of dual polarization radar, the errors of Methods 2 and 3 have been significantly reduced. Among them, the QPE product of Method 3 had a 13.5% lower evaluation of the measured precipitation of regional automatic weather stations, which was 31.1% higher than Method 1. It indicated that polarization parameters could optimize the ZR relationship between reflectivity factor and rainfall intensity (Method 1). From the perspective of *Bias*, all three methods showed slightly positive bias. *Bias* of Method 1 was 0.554, as shown in Fig. 2a. *Bias* of Method 2 was 0.692, as shown in Fig. 2b. *Bias* of Method 3 was 0.865, as shown in Fig. 2c. However, these biases can be ignored in the overall precipitation assessment.

In summary, by comparing three methods, the optimized Method 3 using polarization parameters of horizontal reflectivity (Z_H) and differential reflectivity (Z_{DR}) had smaller errors than Methods 1 and 2 in the quantitative estimation of precipitation by Guigang X-band radar. The QPE product had higher consistency with the measured precipitation by regional automatic weather stations. Among them, Method 3 has been improved by 31.1% compared to Method 1 and 17.3% compared to Method 2. In this paper, Method 3 was used to evaluate the quantitative estimation of precipitation by Guigang X-band radar.

2.3 QPE algorithm evaluation In this paper, the QPE products of the Nanning S-band radar and the Yulin S-band radar were used to compare, which were the closest to the X band of Guigang. The Nanning S-band radar is located about 120 km southwest of the Guigang X-band radar, while the Yulin S-band radar is located about 80 km southeast of the Guigang X-band radar. The QPE products of the Nanning and Yulin S-band radars were compared with the actual rainfall measured by the automatic weather station to evaluate the quantitative precipitation estimation error of the Guigang X-band radar. In this paper, the QPE products within the same detection range of three radars were used to compare and evaluate with the measured precipitation from automatic weather stations.

In this paper, QPE products in June and July 2023 were also selected, and a total of 14 925 sample data pairs were analyzed, as shown in Fig. 3. From Fig. 3a, it can be seen that CC of the Guigang X-band radar was 0.681, with high dispersion and low consistency. The correlation between the QPE product and the measured precipitation of the regional automatic weather station was low. CC of the Nanning S-band radar was 0.944, as shown in Fig. 3b. CC of the Yulin S-band radar was 0.894, as shown in Fig. 3c. For a long period of time, the QPE of the Nanning S-band radar had a good correlation with the measured precipitation of the automatic weather station. *RMSE* of Guigang X-band radar was 6.036, as shown in Fig. 3a. *RMSE* of Nanning S-band radar was 2.678, as shown in Fig. 3b. RMSE of Yulin S-band radar was 3.625, as shown in Fig. 3c. The QPE product of Nanning S-band radar had the smallest error compared to the measured precipitation at the regional automatic meteorological observation station. *RMB* of the Guigang X-band radar was –16.4%, as shown in Fig. 3a. *RMB* of the Nanning S-band radar was 2.7%, as shown in Fig. 3b. RMB of the Yulin S-band radar was –2.6%, as

shown in Fig. 3c. It can be seen that the QPE products of the three radars showed varying degrees of deviation from the measured precipitation of automatic weather observation stations. The QPE product of the Guigang X-band radar underestimated the measured precipitation more, while the S-band radar of Nanning overestimated the measured precipitation by 2.7%. The QPE product of the Yulin S-band radar underestimated the measured precipitation of automatic weather stations by 2.6%. From the perspective of *Bias*, *Bias* of the X-band radar in Guigang was 0.836, as shown in Fig. 3a. Bias of the S-band radar in Nanning was 1.027, as shown in Fig. 3b. Bias of the S-band radar in Yulin was 0.974, as shown in Fig. 3c. The systematic bias of the S-band radar in Nanning was the largest.

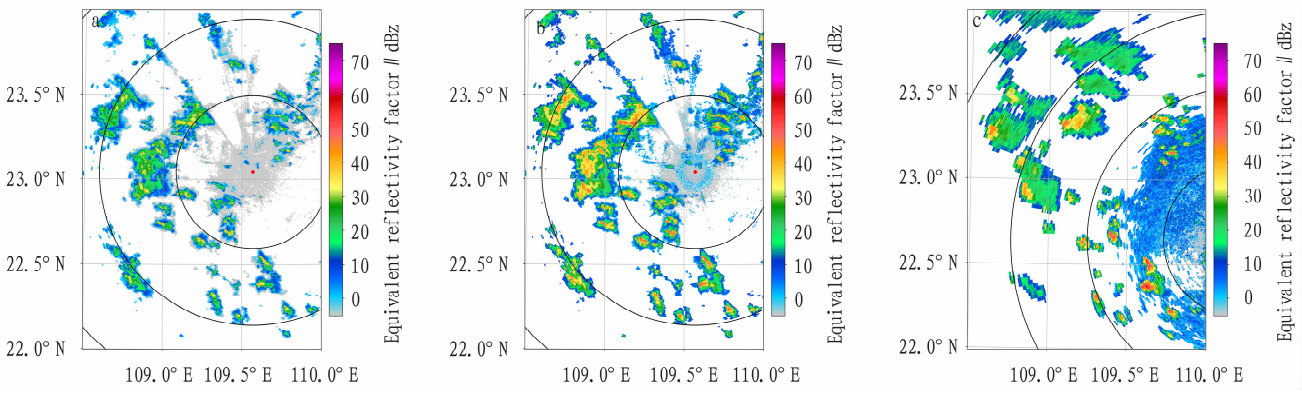

Note: a. Original reflectivity factor of Guigang X-band radar; b. Revised reflectivity factor of Guigang X-band radar; c. Reflectivity factor of Yulin S-band radar during the same period.

Fig. 1 Comparison of reflectance factor attenuation correction and ground object echo correction results

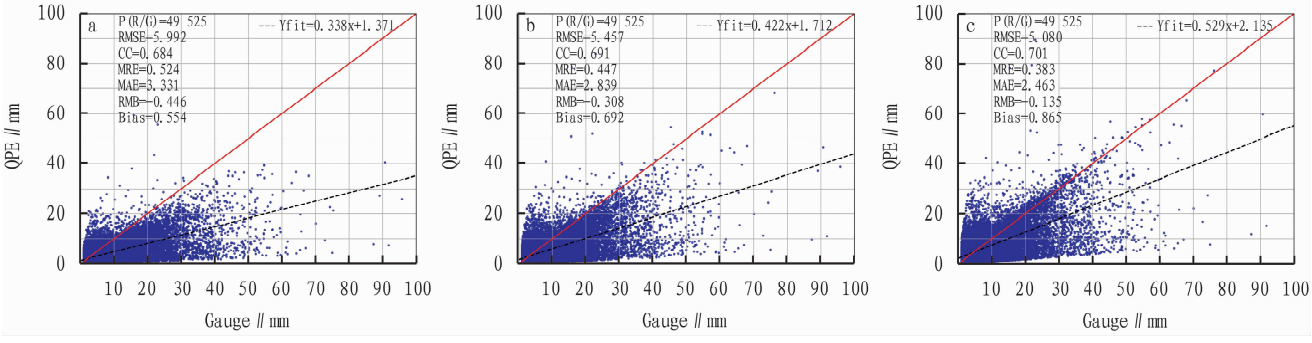

Note: a. $R(Z_H)$; b. $R(K_{DP})$; c. $R(Z_H, Z_{DR})$.

Fig. 2 Comparative scatter distribution chart between hourly estimated precipitation using three QPE algorithms with measured precipitation from regional automatic weather stations

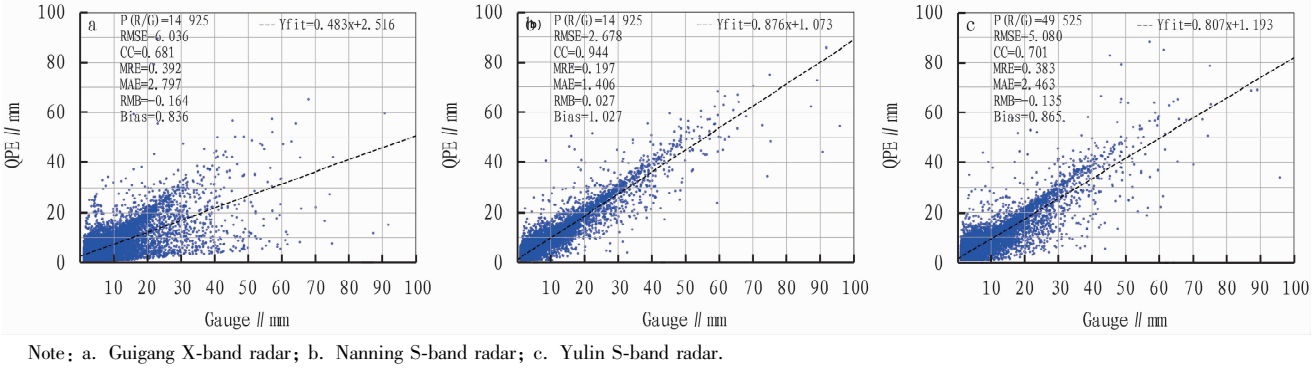

Note: a. Guigang X-band radar; b. Nanning S-band radar; c. Yulin S-band radar.

Fig. 3 Comparative scatter distribution chart between the estimated precipitation of QPE products and the measured precipitation of regional automatic weather stations in June and July 2023

Fig. 4a showed the variation of QPE accuracy *RMSE* curves for each azimuth interval of the three radars in June and July 2023. Fig. 4b showed the variation of QPE accuracy curves with increasing radar distance during the same period. From Fig. 4a1, it can be seen that for long-term precipitation processes, *RMSE* of the QPE product accuracy of Guigang X-band radar in the north

and south directions was relatively large, with a deviation of 6 – 10. *RMSE* in the east direction was 4 – 6, and *RMSE* in most other directions was between 2 – 4. From Fig. 4a2, it can be seen that *RMSE* of the Nanning S-band radar in all directions was mostly between 2 – 4, but there was obstruction in the northwest direction, resulting in blind spots. From Fig. 4a3, it can be seen that the Yulin S-band radar had a large *RMSE* in the north and southwest directions, with a *RMSE* between 4 – 6, and *RMSE* in other directions was approximately 2 – 4. From Fig. 4b1, it can be seen that for the QPE prediction product of precipitation process in June and July 2023, *RMSE* of Guigang X-band radar was the smallest at 30 – 60 km, about 3.5, and gradually increased above 60 km. From Fig. 4b2, it can be seen that for the S-band radar in Nanning, *RMSE* of QPE product from 0 to < 60 km was relatively small and gradually increased with distance. For the Yulin S-band radar (Fig. 4b3), *RMSE* of QPE product with a range of 0 – 30 km was the smallest, and the accuracy error increased significantly with increasing distance.

Fig. 5 showed the error comparison of QPE products with different intensities of rainfall in June and July 2023. As shown in Fig. 5, the smaller the rainfall, the smaller the *RMSE* of QPE products. When rainfall was from 0 to 50 mm/h, *RMSE* of QPE products for Nanning S-band and Yulin S-band radars was comparable, while *RMSE* of QPE product for Guigang X-band radar was the highest. When the rainfall exceeded 50 mm/h, *RMSE* of the three radars increased significantly. Among them, *RMSE* increase of the S-band radar in Nanning was relatively small, while *RMSE* of the X-band radar in Guigang increased significantly. This indicated that the prediction of heavy rainfall exceeding 50 mm/h by Guigang X-band radar was not as good as that of the S-band radars in Nanning and Yulin. Comparing the QPE products for different intensities of rainfall during the long period of June to July 2023, it was found that the Nanning S-band radar had the smallest QPE product error, followed by the Yulin S-band radar.

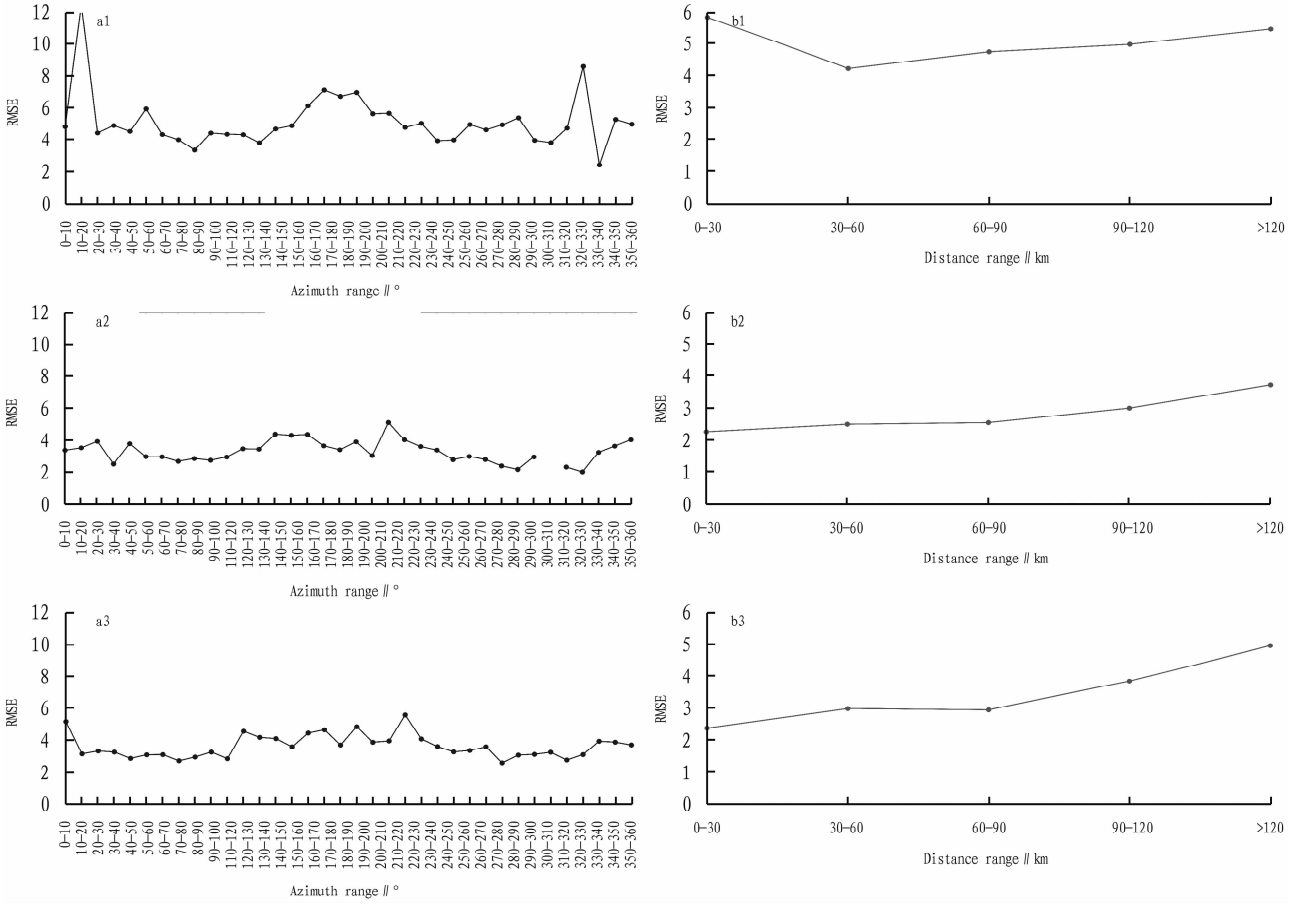

Note: a1. Guigang X-band radar; b1. Nanning S-band radar; c1. Yulin S-band radar; a2. Guigang X-band radar; b2. Nanning S-band radar; c2. Yulin S-band radar.

Fig. 4 *RMSE* curve variation of QPE product accuracy in each azimuth interval (a) with radar distance increase (b)

In summary, *RMSE* values of the three radars fluctuated in different time periods for the data during this period. *RMSE* values of the X-band radar in Guigang, the S-band radar in Nanning, and the S-band radar in Yulin were 6.036, 2.678, and 3.625. Overall, they remained within a reasonable range, demonstrating the effective estimation of precipitation by the radars. *CC* values of the three radars remained relatively stable during the analysis period, indicating that the radar data had high accuracy in capturing the trend of precipitation changes. For 14 925 samples, *RMB* values of the three radars were slightly different, with the Guigang X-band

radar being -0.164, the Nanning S-band radar being 0.027, and the Yulin S-band radar being -0.026. However, the overall bias was within an acceptable range, indicating its good practicality. *Bias* is used to quantify the systematic deviation between estimated values and actual values. *Bias* values of Guigang X-band radar, Nanning S-band radar, and Yulin S-band radar were 0.836, 1.027, and 0.974. *Bias* values of the three radars showed slightly positive bias, but these biases can be basically ignored in the overall precipitation assessment. Overall, Nanning S-band radar was the best in terms of QPE, followed by Yulin S-band radar. Guigang X-band radar was slightly inferior to Nanning and Yulin S-band radars in QPE. In terms of quantitative precipitation estimation, X-band radar is still slightly inferior to S-band radar due to significant attenuation.

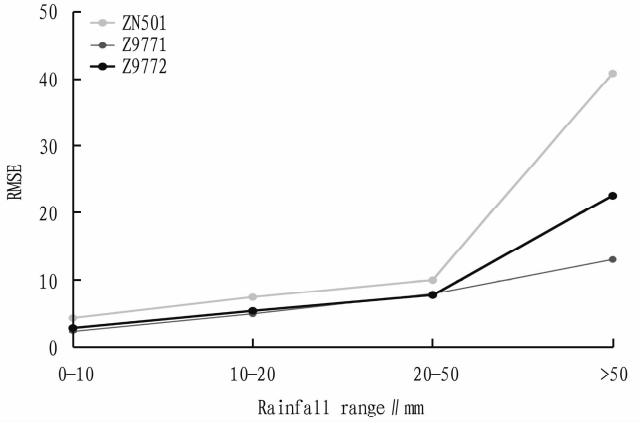

Fig. 5 Comparison of QPE product errors using three radars for rainfall of different intensities

3 Conclusions

(1) Rain area attenuation correction and ground object echo suppression of Guigang X-band dual polarization radar were conducted, and three radar estimation methods for precipitation were evaluated. By comparing the three methods, the optimized Method 3 using polarization parameters of horizontal reflectivity (Z_H) and differential reflectivity (Z_{DR}) showed smaller errors in quantitative estimation of precipitation of the Guigang X-band radar compared to Methods 1 and 2. The QPE product showed higher consistency with the measured precipitation at the regional automatic weather station. Among them, Method 3 was improved by 31.1% compared to Method 1 and 17.3% compared to Method 2.

(2) QPE results of precipitation processes affecting Guigang City were objectively analyzed using Guigang X-band radar and surrounding Nanning and Yulin S-band radars. By evaluating the correlation coefficient CC, root mean square error *RMSE*, relative average error *RMB*, system deviation *Bias* and other indicators, the three radars performed stably in the evaluation. *RMSE* of the quantitative estimation of precipitation by the three radars remained within a reasonable range, indicating that the radar's estimation results of precipitation were relatively reliable. Overall, in terms of quantitative estimation of precipitation, Nanning S-band radar was the best, followed by Yulin S-band radar, and Guigang X-band radar was slightly inferior to Nanning and Yulin S-band radars.

Overall, these indicators provided a reliable basis for evaluating the accuracy and applicability of QPE products using Guigang X-band radar. In the future, data from different bands of radar (such as S-band and X-band) can be combined to fully utilize the penetration capability of S-band and the high-resolution advantage of X-band. Through data fusion technology, the accuracy of QPE products by Guigang X-band radar can be improved.

References

[1] LIU LP, QIAN YF, WANG ZJ, *et al*. Comparative study on dual linear polarization radar measuring rainfall rate[J]. Chinese Journal of Atmospheric Sciences, 1996, 20(5): 615-619.

[2] XUN AP, ZHANG W, HUANG HR, *et al*. Analysis of rainfall measuring errors of S-band dual polarization weather radar in Xiamen[J]. Meteorological and Environmental Sciences, 2019, 42(4): 103-110.

[3] YU XD, YAO XP, XIONG TN, *et al*. Principles and business applications of Doppler weather radar[M]. Beijing: China Meteorological Press, 2006.

[4] ZHANG PC. Radar meteorology[M]. Beijing: China Meteorological Press, 2001.

[5] ZHANG Z, QI YC, ZHU ZW, *et al*. Application of radar quantitative precipitation estimation using S-band and X-band polarimetric radars in Shenzhen[J]. Acta Meteorologica Sinica, 2021, 79(5): 786-803.

[6] ZHANG WR, WU C, LIU LP, *et al*. Research on quantitative comparison and observation precision of dual polarization phased array radar and operational radar[J]. Plateau Meteorology, 2021, 40(2): 424-435.

[7] ZHANG Y, WU SF, LI HW, *et al*. Data quality analysis and application of Guangzhou X-band dual polarization phased array radars[J]. Journal of Tropical Meteorology, 2022, 38(1): 23-34.

[8] ZHANG PC, DAI TP, WANG DY, *et al*. Derivation of the Z-I relationship by optimization and the accuracy in the quantitative rainfall measurement[J]. Journal of the Meteorological Sciences, 1992(3): 6.

[9] ZHENG YY, XIE YF, WU LL, *et al*. Comparative experiment with several quantitative precipitation estimator techniques based on Doppler radar over the Huaihe valley during rainy season[J]. Journal of Tropical Meteorology, 2004, 20(2): 192-197.

[10] LIU LP, WANG ZJ, XU BX, *et al*. Study on theory and application of dual-polarization radar in China[J]. Plateau Meteorology, 1997, 16(1): 99-104.

[11] ZHANG PC, WEI M, HUANG XY, *et al*. Detection principle and application of dual polarization Doppler weather radar[M]. Beijing: China Meteorological Press, 2018.

[12] ZHANG Z, QI YC, LAN HP, *et al*. Introduction to a radar mosaicking system for quantitative precipitation estimation based on the S-band and X-band phase-array polarimetric radars in Shenzhen[J]. Acta Meteorologica Sinica, 2023, 81(3): 506-519.

[13] MEI YF, CHEN S, LIU CS, *et al*. Quality evaluation of X-band polarimetric phased array radar QPE product in Zhuhai[J]. Journal of Tropical Meteorology, 2023, 39(4): 614-621.

[14] XUN AP, ZHAO YC, LI F, *et al*. Analysis of radar quantitative precipitation estimation using X-band polarimetric radar[J]. Torrential Rain and Disasters, 2023, 42(4): 437-445.

[15] ALEXANDER VR, DUSAN SZ. Radar polarimetry for weather observations[M]. Springer Nature Swizerland AG, 2019.

[16] BRINGI VN, CHANDRASEKAR V, BALAKRISHNAN N, *et al*. An examination of propagation effects in rainfall on polarimetric variables at microwave frequencies[J]. Atmos Oceanic Technol, 1990,7: 829-840.

[17] MATROSOV SY, CLARK KA, MARTNER BE. X-band polarimetric radar measurements of rainfall[J]. Appl Meteor, 2002, 41: 941-952.

[18] PARK SG, BRINGI VN, CHANDRASEKAR V, *et al*. Correction of radar reflectivity and differential reflectivity for rain attenuation at X-band. Part I: Theoretical and empirical basis[J]. Atmos Oceanic Technol, 2005, 22: 1621-1632.